

# Phase-averaged equation for water waves

Odin Gramstad<sup>1,†</sup> and Michael Stiassnie<sup>2</sup>

<sup>1</sup>Department of Mathematics, University of Oslo, PO Box 1053 Blindern, NO-0316 Oslo, Norway

<sup>2</sup>Faculty of Civil and Environmental Engineering, Technion IIT, Haifa 32000, Israel

(Received 19 December 2011; revised 23 November 2012; accepted 7 December 2012;  
first published online 8 February 2013)

We investigate phase-averaged equations describing the spectral evolution of dispersive water waves subject to weakly nonlinear quartet interactions. In contrast to Hasselmann's kinetic equation, we include the effects of near-resonant quartet interaction, leading to spectral evolution on the 'fast'  $O(\epsilon^{-2})$  time scale, where  $\epsilon$  is the wave steepness. Such a phase-averaged equation was proposed by Annenkov & Shrira (*J. Fluid Mech.*, vol. 561, 2006*b*, pp. 181–207). In this paper we rederive their equation taking some additional higher-order effects related to the Stokes correction of the frequencies into account. We also derive invariants of motion for the phase-averaged equation. A numerical solver for the phase-averaged equation is developed and successfully tested with respect to convergence and conservation of invariants. Numerical simulations of one- and two-dimensional spectral evolution are performed. It is shown that the phase-averaged equation describes the 'fast' evolution of a spectrum on the  $O(\epsilon^{-2})$  time scale well, in good agreement with Monte-Carlo simulations using the Zakharov equation and in qualitative agreement with known features of one- and two-dimensional spectral evolution. We suggest that the phase-averaged equation may be a suitable replacement for the kinetic equation during the initial part of the evolution of a wave field, and in situations where 'fast' field evolution takes place.

**Key words:** surface gravity waves, waves/free-surface flows

---

## 1. Introduction

The dominance of quartet interactions in the weakly nonlinear evolution of surface gravity waves was first established by Phillips (1960). The quartet interaction serves as a building brick in almost any model dealing with spectral evolution. The present work is based on Zakharov's equation (Zakharov 1968) for the temporal evolution of the complex amplitude spectrum  $b(\mathbf{k}, t)$ , where  $\mathbf{k}$  is the wavenumber vector and  $t$  is time. Zakharov's equation is deterministic, i.e. no stochastic assumptions were made in the course of its derivation, and it is phase resolving, i.e. it describes the evolution of the phases of the waves.

Earlier Hasselmann (1962) derived an equation for the nonlinear evolution of the wave-action spectrum  $C(\mathbf{k}, t) = \langle |b(\mathbf{k}, t)|^2 \rangle$ , where  $\langle \cdot \rangle$  denotes the statistical

<sup>†</sup> Email address for correspondence: [oding@math.uio.no](mailto:oding@math.uio.no)

average (expectation). Equations of this type, describing the evolution of certain statistical properties of a random wave field appear in many different fields of physics where weakly nonlinear dispersive waves are present. In the context of water waves this equation is often referred to as the Hasselmann equation or the kinetic equation. Here we will use the latter term. The kinetic equation serves as the main mathematical model for describing the statistical evolution of random waves due to weakly nonlinear quartet interactions. It is the theoretical framework for the theory of wave turbulence, see Zakharov, L'vov & Falkovich (1992) and references therein, which has established important concepts about the energy transfer within the wave spectrum. The kinetic equation is also the core part of operational wave forecasting models.

In the derivation of the kinetic equation certain assumptions about the stochastic properties of the system are necessary. These include: (i) the assumption that the wave process is nearly Gaussian; (ii) the assumption that the phases of the waves were uncorrelated at some instant  $t_0$ ; and (iii) that this instant occurred sufficiently long time ago (formally  $t - t_0 \rightarrow \infty$ ) to enable a certain time scale separation. Details about application of these concepts to the Zakharov equation in order to derive from it the kinetic equation can be found in e.g. Zakharov *et al.* (1992) and Janssen (2004). See also the [Appendix](#). The kinetic equation does not include information about modal phases and is in this sense a phase-averaged equation. The nonlinear energy transfer in the kinetic equation occurs at a rather slow time scale so that the rate of change of the action density  $C$  is proportional to  $C^3$ . Hence,

$$\frac{1}{C} \frac{\partial C}{\partial t} = O(\epsilon^4 \omega_0), \quad (1.1)$$

where  $\epsilon$  is the wave steepness and  $\omega_0$  is a typical frequency of the wave field. Thus, the evolution takes place on an  $O(\epsilon^{-4})$  time scale. An important point is that assumption (iii) above, which is made in the derivation of the kinetic equation, averages out the contribution from the near-resonance quartets and maintains only quartets in exact resonance. It is worth noting that since there are no exact resonance quartets for waves in one horizontal dimension (Dyachenko & Zakharov 1994), the kinetic equation predicts no change of a one-dimensional spectrum.

Although the kinetic equation is unable to describe evolution on faster time scales, it is clear that in nature faster evolution may occur for various reasons. It is quite well known that a wave field which is initially far from an equilibrium state will evolve on the  $O(\epsilon^{-2})$  time scale during initial stages of the evolution. This is for example seen in numerical Monte-Carlo simulations of deterministic equations, where phases are chosen randomly at  $t = 0$  (Dysthe *et al.* 2003; Stiassnie & Shemer 2005; Annenkov & Shrira 2006a). Moreover, Annenkov & Shrira (2009) showed by direct numerical simulations of the Zakharov equation that fast spectral evolution is expected to occur as a result of any strong perturbation of the wave field, for example as a result of an abrupt change of forcing due to wind. This is also supported by field observations and experiments showing fast nonlinear evolution of wave fields as a result of rapid changes in wind speed or direction (van Vledder & Holthuijsen 1993; Waseda, Toba & Tulin 2001). It is clear that the kinetic equation is inadequate for describing such situations where the nonlinear energy transfer takes place on the fast  $O(\epsilon^{-2})$  time scale.

The importance of near-resonant quartet interactions in nonlinear evolution, was also noted by Janssen (2003), who suggested a modification to the kinetic equation which includes effects of non-resonant interactions. By comparison with Monte-Carlo simulation of the nonlinear Schrödinger equation and the Zakharov equation he found

good agreement with his modified kinetic equation for evolution of one-dimensional spectra. Later, Annenkov & Shrira (2006b) proposed a more general phase-averaged equation, which describes the spectral evolution on the  $O(\epsilon^{-2})$  time scale. To our knowledge no real applications of such a modified kinetic equation have been presented. This is however the main purpose of the present paper.

The derivation of the modified kinetic equation, which in the following we will refer to as the phase-averaged equation (PAE), is given in § 2. The equation is derived starting from the Zakharov equation and follows roughly the same procedure as in the derivation given by Annenkov & Shrira (2006b). However, compared to Annenkov & Shrira (2006b) we include some additional higher-order contributions in the statistical closure. The derivation shares many of the same concepts as the derivation of the kinetic equation, but uses more relaxed stochastic properties. More specifically we assume: (i) a nearly Gaussian and weakly nonlinear process; and (ii) that the modal phases are uncorrelated at  $t = 0$ . The PAE has certain invariants of motion, which are derived in § 3.

The rest of the paper presents results from numerical simulations with the PAE. The numerical method and simulation setup used to solve the PAE numerically is outlined in § 4. To test and build some confidence in the numerical solver, some validation tests are presented in § 5. We have shown convergence of the numerical solutions with decreasing integration time step as well as checked the accuracy of the invariants derived in § 3. In § 6 we consider the evolution of one-dimensional spectra. We have compared the results from the PAE with results obtained from Monte–Carlo simulations using the Zakharov equation directly. The results show in general a good agreement between the PAE and direct simulations with the Zakharov equation, and confirm the importance of evolution on the  $O(\epsilon^{-2})$  time scale, which is in sharp contrast to the standard kinetic equation which predicts no change of a one-dimensional spectrum.

Spectral evolution of more realistic two-dimensional spectra are considered in § 7. Also here our results clearly show the importance of the fast initial evolution of a spectrum. Good agreement is found between the spectral evolution obtained from the PAE and from Monte–Carlo simulations with the Zakharov equation.

In § 8 we discuss how mixing of the phases at certain chosen times during the evolution of a wave field affects the spectral evolution. This might be relevant if there exists some physical process that mixes phases with certain intervals. It is suggested that strong wave breaking might have such an effect (Babanin *et al.* 2007, 2010). Finally, discussion and conclusions are given in § 9.

## 2. Derivation of phase-averaged equations

Our starting point is the Zakharov equation (Zakharov 1968) for the generalized complex amplitude spectrum  $b(\mathbf{k}, t)$

$$\begin{aligned} i \frac{\partial b(\mathbf{k})}{\partial t} = & \omega(\mathbf{k})b(\mathbf{k}) + \int T(\mathbf{k}, \mathbf{k}_1, \mathbf{k}_2, \mathbf{k}_3) b^*(\mathbf{k}_1) b(\mathbf{k}_2) b(\mathbf{k}_3) \\ & \times \delta(\mathbf{k} + \mathbf{k}_1 - \mathbf{k}_2 - \mathbf{k}_3) d\mathbf{k}_1 d\mathbf{k}_2 d\mathbf{k}_3. \end{aligned} \quad (2.1)$$

Here  $t$  is time,  $\mathbf{k}$  is the wavenumber vector and  $\omega(\mathbf{k}) = \sqrt{g|\mathbf{k}| \tanh(|\mathbf{k}|h)}$  is the frequency,  $g$  is the acceleration due to gravity,  $h$  is the water depth and asterisk denotes complex conjugation. Details about the kernel function  $T(\mathbf{k}, \mathbf{k}_1, \mathbf{k}_2, \mathbf{k}_3)$  can be found in e.g. Krasitskii (1994) and Mei, Stiassnie & Yue (2005).

If assuming a discrete spectrum

$$b(\mathbf{k}, t) = \sum_n b_n(t) \delta(\mathbf{k} - \mathbf{k}_n), \quad (2.2)$$

the Zakharov equation is replaced by the system

$$\frac{db_n}{dt} = -i\omega_n b_n - i \sum_{p,q,r} T_{npqr} b_p^* b_q b_r \delta_{np}^{qr}, \quad (2.3)$$

where  $T_{npqr} = T(\mathbf{k}_n, \mathbf{k}_p, \mathbf{k}_q, \mathbf{k}_r)$ ,  $\omega_n = \omega(\mathbf{k}_n)$  and  $\delta_{np}^{qr}$  is the Kronecker delta

$$\delta_{np}^{qr} = \begin{cases} 1 & \text{when } \mathbf{k}_n + \mathbf{k}_p = \mathbf{k}_q + \mathbf{k}_r, \\ 0 & \text{otherwise.} \end{cases} \quad (2.4)$$

One should note that (2.3) is based on a naive discretization of the Zakharov equation. A more sophisticated discretization is proposed in Gramstad, Agnon & Stiassnie (2011), but its stochastic counterpart is expected to be very cumbersome.

We now assume that  $b_j$  are stochastic processes and let  $\langle \cdot \rangle$  denote the statistical average (the expectation). Multiplying (2.3) by  $b_n^*$ , adding the result to its complex conjugate and averaging gives the equation

$$\frac{dC_n}{dt} = -i \sum_{p,q,r} T_{npqr} (\langle b_n^* b_p^* b_q b_r \rangle - \langle b_r^* b_q^* b_p b_n \rangle) \delta_{np}^{qr} = 2\text{Im} \sum_{p,q,r} T_{npqr} \langle b_n^* b_p^* b_q b_r \rangle \delta_{np}^{qr}, \quad (2.5)$$

where  $C_n = \langle |b_n|^2 \rangle$  is the wave action. To obtain an equation for the fourth-order moment we differentiate the product  $b_n^* b_p^* b_q b_r$  with respect to time and substitute from (2.3). This gives

$$\begin{aligned} \frac{d}{dt} \langle b_n^* b_p^* b_q b_r \rangle &= i \Delta_{np}^{qr} \langle b_n^* b_p^* b_q b_r \rangle \\ &+ i \sum_{u,v,w} T_{nuvw} \langle b_p^* b_v^* b_w^* b_q b_r b_u \rangle \delta_{nu}^{vw} + i \sum_{u,v,w} T_{puvw} \langle b_n^* b_v^* b_w^* b_q b_r b_u \rangle \delta_{pu}^{vw} \\ &- i \sum_{u,v,w} T_{quvw} \langle b_n^* b_p^* b_u^* b_r b_v b_w \rangle \delta_{qu}^{vw} - i \sum_{u,v,w} T_{ruvw} \langle b_n^* b_p^* b_u^* b_q b_v b_w \rangle \delta_{ru}^{vw}, \end{aligned} \quad (2.6)$$

where

$$\Delta_{np}^{qr} = \omega_n + \omega_p - \omega_q - \omega_r. \quad (2.7)$$

We now invoke the usual assumptions of statistical homogeneity and weak non-Gaussianity. One can express the averages in the following forms (see e.g. Lvov, Binder & Newell 1998):

$$\langle b_n^* b_p \rangle = C_n \delta_n^p, \quad (2.8a)$$

$$\langle b_n^* b_p^* b_q b_r \rangle = C_n C_p (\delta_n^q \delta_p^r + \delta_n^r \delta_p^q) + k_{npqr}, \quad (2.8b)$$

$$\begin{aligned} \langle b_n^* b_p^* b_q^* b_r b_u b_v \rangle &= C_n C_p C_q (\delta_n^r \delta_p^u \delta_q^v + \delta_n^r \delta_p^v \delta_q^u + \delta_n^u \delta_p^r \delta_q^v + \delta_n^u \delta_p^v \delta_q^r + \delta_n^v \delta_p^r \delta_q^u + \delta_n^v \delta_p^u \delta_q^r) \\ &+ C_n (k_{pquv} \delta_n^r \delta_{pq}^{uv} + k_{pqr v} \delta_n^u \delta_{pq}^{rv} + k_{pqru} \delta_n^v \delta_{pq}^{ru}) \\ &+ C_p (k_{nquv} \delta_p^r \delta_{nq}^{uv} + k_{nqr v} \delta_p^u \delta_{nq}^{rv} + k_{nqru} \delta_p^v \delta_{nq}^{ru}) \\ &+ C_q (k_{npuv} \delta_q^r \delta_{np}^{uv} + k_{npr v} \delta_q^u \delta_{np}^{rv} + k_{npru} \delta_q^v \delta_{np}^{ru}) + k_{npqr uv}. \end{aligned} \quad (2.8c)$$

Here,

$$\delta_n^p = \begin{cases} 1 & \text{when } \mathbf{k}_n = \mathbf{k}_p, \\ 0 & \text{otherwise,} \end{cases} \quad (2.9)$$

and  $k_{npqr}$  and  $k_{npqruv}$  are the fourth- and sixth-order joint cumulants, respectively, which are assumed to be small under the assumption of weak non-Gaussianity. Substituting (2.8b) into (2.5) gives

$$\frac{dC_n}{dt} = -i \sum_{p,q,r} T_{npqr} (k_{npqr} - k_{rqpn}) \delta_{np}^{qr} = 2\text{Im} \sum_{p,q,r} T_{npqr} k_{npqr} \delta_{np}^{qr}. \quad (2.10)$$

Similarly, (2.8b) into (2.6) gives

$$\begin{aligned} \frac{d}{dt} k_{npqr} &= i \Delta_{np}^{qr} k_{npqr} - \frac{d}{dt} C_n C_p (\delta_n^q \delta_p^r + \delta_n^r \delta_p^q) \\ &+ i \sum_{u,v,w} T_{nuvw} \langle b_p^* b_v^* b_w^* b_q b_r b_u \rangle \delta_{nu}^{vw} + i \sum_{u,v,w} T_{puvw} \langle b_n^* b_v^* b_w^* b_q b_r b_u \rangle \delta_{pu}^{vw} \\ &- i \sum_{u,v,w} T_{quvw} \langle b_n^* b_p^* b_u^* b_r b_v b_w \rangle \delta_{qu}^{vw} - i \sum_{u,v,w} T_{ruvw} \langle b_n^* b_p^* b_u^* b_q b_v b_w \rangle \delta_{ru}^{vw}. \end{aligned} \quad (2.11)$$

Closure of the system (2.10)–(2.11) relies on the assumptions that the wave field is weakly nonlinear and obeys weakly non-Gaussian statistics. The assumption of weak non-Gaussianity has the consequence that the fourth- and sixth-order cumulants are smaller than terms of the same nonlinear order involving  $C_n$ . These assumptions may lead to the following ordering:

$$C_n = O(\epsilon^2), \quad k_{npqr} = o(\epsilon^4), \quad k_{npqruv} = o(\epsilon^6), \quad (2.12)$$

where  $\epsilon \ll 1$  is the wave steepness. Below we discuss the closure of (2.10)–(2.11) to different orders of  $\epsilon$ . First, we note that ignoring terms of  $o(\epsilon^4)$  in (2.10)–(2.11) leads to the trivial result  $dC_n/dt = 0$ , which shows that to leading order only the phases of the wave field change. To next order, including terms of  $o(\epsilon^4)$  but ignoring terms of  $o(\epsilon^6)$ , only the first line in (2.8c) is significant. In this case one can show that (2.11) takes the form

$$\frac{d}{dt} k_{npqr} = i[\alpha_{npqr} + \Delta_{np}^{qr} k_{npqr}], \quad (2.13)$$

where

$$\alpha_{npqr} = 2T_{npqr} \delta_{np}^{qr} [C_q C_r (C_n + C_p) - C_n C_p (C_q + C_r)]. \quad (2.14)$$

If we further also include the terms in (2.8c) that involve the fourth-order cumulants, (2.11) has an additional contribution and takes the form

$$\frac{d}{dt} k_{npqr} = i[\alpha_{npqr} + (\Delta_{np}^{qr} + \beta_{npqr}) k_{npqr}], \quad (2.15)$$

where

$$\beta_{npqr} = 2 \sum_u C_u (T_{nuvu} + T_{pupu} - T_{ququ} - T_{ruvu}). \quad (2.16)$$

Note that (2.15) is strictly mathematically consistent only if one assumes that the sixth-order cumulant is smaller than products of  $C_n$  and fourth-order cumulants. Note

further that to this order, effects from quintet interactions described by modifications to the Zakharov equation (Stiassnie & Shemer 1984; Krasitskii 1994) may also be significant. Since we here start out from the standard (four-wave) Zakharov equation, effects from quintet interactions are not included in our derivation.

From (2.16) one sees that  $\beta_{npqr}$  incorporates the nonlinear Stokes corrections of the frequencies, which actually cause resonating wave quartets to lose the resonance property during their evolution in time. We wish to include this effect in order to see to what extent this affects the spectral evolution. Note that while phase-averaged equations including the effect of  $\beta_{npqr}$  to our knowledge have not been discussed within the field of water waves, similar equations have been presented in other fields of physics (see e.g. Lvov *et al.* 1998).

The general solution of (2.13) and (2.15) can be written

$$k_{npqr}(t) = \left[ k_{npqr}(0) + i \int_0^t \alpha_{npqr}(\tau) e^{-i\theta_{npqr}(\tau)} d\tau \right] e^{i\theta_{npqr}(t)}, \quad (2.17)$$

where

$$\theta_{npqr}(t) = \Delta_{np}^{qr} t, \quad (2.18a)$$

or

$$\theta_{npqr}(t) = \Delta_{np}^{qr} t + \int_0^t \beta_{npqr}(\xi) d\xi, \quad (2.18b)$$

to  $O(\epsilon^5)$  and  $O(\epsilon^7)$  respectively.

Assuming a Gaussian initial condition such that  $k_{npqr}(0) = 0$ , (2.17) and (2.14) substituted into (2.10) gives the equation

$$\frac{dC_n}{dt} = 4\text{Re} \sum_{p,q,r} T_{npqr}^2 \delta_{np}^{qr} e^{i\theta_{npqr}(t)} \int_0^t f_{npqr}(\tau) e^{-i\theta_{npqr}(\tau)} d\tau, \quad (2.19a)$$

where

$$f_{npqr} = C_q C_r (C_n + C_p) - C_n C_p (C_q + C_r). \quad (2.19b)$$

Equation (2.19a), which we will refer to as the PAE, is proposed as a possible alternative to the standard kinetic equation for water waves (Hasselmann 1962). The main advantage of the PAE compared to the standard kinetic equation is its ability to describe spectral evolution on the relatively fast  $O(\epsilon^{-2})$  time scale. The PAE with  $\beta_{npqr} = 0$  has previously been presented by Annenkov & Shrira (2006b).

### 3. Invariants

In the following we show that the PAE (2.19a) conserves the following three quantities:

$$\tilde{N} = \sum_n C_n, \quad (3.1a)$$

$$\tilde{P} = \sum_n \mathbf{k}_n C_n, \quad (3.1b)$$

$$\tilde{H} = \sum_n \Omega_n C_n - \sum_{n,p,q,r} T_{npqr}^2 \text{Im} \left( e^{i\theta_{npqr}(t)} \int_0^t f_{npqr}(\tau) e^{-i\theta_{npqr}(\tau)} d\tau \right) \delta_{np}^{qr}, \quad (3.1c)$$

where  $\Omega_n = \omega_n$  if  $\theta_{npqr}$  is given by (2.18a) and  $\Omega_n = \omega_n + \sum_u T_{nunu} C_u$  if  $\theta_{npqr}$  is given by (2.18b). One can show that (3.1) are the statistically averaged versions of the invariants for the Zakharov equation: the wave action, momentum and Hamiltonian, respectively.

In order to show that (3.1) are conserved by the PAE, it is convenient to write the PAE (2.19a) in the form

$$\frac{dC_n}{dt} = \sum_{p,q,r} M_{npqr} \delta_{np}^{qr}, \tag{3.2a}$$

where

$$M_{npqr} = 4T_{npqr}^2 \operatorname{Re} \left( e^{i\theta_{npqr}(t)} \int_0^t f_{npqr}(\tau) e^{-i\theta_{npqr}(\tau)} d\tau \right). \tag{3.2b}$$

One can show that  $M_{npqr} = M_{pnqr} = M_{nprq} = -M_{qmp}$ . By straightforward manipulations with the dummy summation indexes one then finds

$$\frac{d\tilde{N}}{dt} = \sum_{n,p,q,r} M_{npqr} \delta_{np}^{qr} = \frac{1}{2} \sum_{n,p,q,r} (M_{npqr} + M_{qmp}) \delta_{np}^{qr} = 0, \tag{3.3a}$$

$$\begin{aligned} \frac{d\tilde{P}}{dt} &= \sum_{n,p,q,r} \mathbf{k}_n M_{npqr} \delta_{np}^{qr} = \frac{1}{4} \sum_{n,p,q,r} (\mathbf{k}_n M_{npqr} + \mathbf{k}_p M_{pnqr} + \mathbf{k}_q M_{qmp} + \mathbf{k}_r M_{rqpn}) \delta_{np}^{qr} \\ &= \frac{1}{4} \sum_{n,p,q,r} (\mathbf{k}_n + \mathbf{k}_p - \mathbf{k}_q - \mathbf{k}_r) M_{npqr} \delta_{np}^{qr} = 0, \end{aligned} \tag{3.3b}$$

which implies that (3.1a) and (3.1b) are conserved by (2.19a). In the same way one sees that

$$\begin{aligned} \frac{d}{dt} \sum_n \Omega_n C_n &= \sum_n \left( \frac{d\Omega_n}{dt} C_n + \Omega_n \frac{dC_n}{dt} \right) = \frac{1}{4} \sum_{n,p,q,r} \theta'_{npqr}(t) M_{npqr} \delta_{np}^{qr} \\ &= \frac{d}{dt} \sum_{n,p,q,r} T_{npqr}^2 \operatorname{Im} \left( e^{i\theta_{npqr}(t)} \int_0^t f_{npqr}(\tau) e^{-i\theta_{npqr}(\tau)} d\tau \right) \delta_{np}^{qr}, \end{aligned} \tag{3.4}$$

which shows that also (3.1c) is an invariant for (2.19a). Here and in the following, prime denotes derivative with respect to time.

#### 4. Numerical setup and implementation

In the following numerical simulation with the PAE we have used a numerical scheme based on the Taylor expansion

$$C_n(t + \Delta t) = C_n(t) + \Delta t C'_n(t) + \frac{\Delta t^2}{2} C''_n(t) + \frac{\Delta t^3}{6} C'''_n(t) + O(\Delta t^4). \tag{4.1}$$

Using that

$$C'_n(t) = 4 \operatorname{Re} \sum_{p,q,r} T_{npqr}^2 \delta_{np}^{qr} e^{i\theta_{npqr}(t)} I(t), \tag{4.2a}$$

$$C''_n(t) = 4 \operatorname{Re} \sum_{p,q,r} T_{npqr}^2 \delta_{np}^{qr} [f_{npqr}(t) + i\theta'_{npqr}(t) e^{i\theta_{npqr}(t)} I(t)], \tag{4.2b}$$

$$C_n'''(t) = 4\text{Re} \sum_{p,q,r} T_{npqr}^2 \delta_{np}^{qr} [f'_{npqr}(t) + (i\theta''_{npqr}(t) - \theta'_{npqr}(t)^2) e^{i\theta_{npqr}(t)} I(t)], \quad (4.2c)$$

leads to the following explicit scheme with local truncation error of  $O(\Delta t^4)$ :

$$\begin{aligned} C_n(t + \Delta t) = & C_n(t) + 4\Delta t \text{Re} \sum_{p,q,r} T_{npqr}^2 \delta_{np}^{qr} \left[ \frac{\Delta t}{2} f_{npqr}(t) + \frac{\Delta t^2}{6} f'_{npqr}(t) \right. \\ & \left. + \left( 1 + \frac{i\Delta t}{2} \theta'_{npqr}(t) + \frac{\Delta t^2}{6} (i\theta''_{npqr}(t) - \theta'_{npqr}(t)^2) \right) I(t) e^{i\theta_{npqr}(t)} \right] \\ & + O(\Delta t^4), \end{aligned} \quad (4.3)$$

where we have defined

$$I(t) = \int_0^t f_{npqr}(\tau) e^{-i\theta_{npqr}(\tau)} d\tau. \quad (4.4)$$

The integral  $I(t)$  can be calculated iteratively, i.e.

$$\begin{aligned} I(t) = & I(t - \Delta t) + \int_{t-\Delta t}^t f_{npqr}(\tau) e^{-i\theta_{npqr}(\tau)} d\tau \\ = & I(t - \Delta t) + \frac{\Delta t}{2} [f_{npqr}(t - \Delta t) e^{-i\theta_{npqr}(t-\Delta t)} + f_{npqr}(t) e^{-i\theta_{npqr}(t)}] + O(\Delta t^3). \end{aligned} \quad (4.5)$$

Similarly,

$$\begin{aligned} \theta_{npqr}(t) = & \theta_{npqr}(t - \Delta t) + \Delta_{np}^{qr} \Delta t + \int_{t-\Delta t}^t \beta_{npqr}(\xi) d\xi \\ = & \theta_{npqr}(t - \Delta t) + \Delta_{np}^{qr} \Delta t + \frac{\Delta t}{2} [\beta_{npqr}(t - \Delta t) + \beta_{npqr}(t)] + O(\Delta t^3). \end{aligned} \quad (4.6)$$

In addition we use that for  $t \geq \Delta t$

$$\theta''_{npqr}(t) = \beta'_{npqr}(t) = \frac{\beta_{npqr}(t) - \beta_{npqr}(t - \Delta t)}{\Delta t} + O(\Delta t), \quad (4.7a)$$

$$f'_{npqr}(t) = \frac{f_{npqr}(t) - f_{npqr}(t - \Delta t)}{\Delta t} + O(\Delta t), \quad (4.7b)$$

while for  $t = 0$ ,  $\beta'_{npqr}(0) = f'_{npqr}(0) = 0$ . Note that the relatively simple expressions for the derivatives (4.2) as well as the simple way to handle the integral  $I(t)$  make the above higher-order one-step explicit scheme convenient. Such higher-order schemes based on Taylor expansions have previously been employed successfully on other problems related to wave propagation (Dold & Peregrine 1986; Cooker *et al.* 1990).

As initial condition for the numerical solver the initial spectral density  $C_n(t = 0)$  is needed. One may choose  $C_n(t = 0)$  according to a desired energy spectrum  $S(\mathbf{k})$  so that  $S_n = C_n \omega_n / g = S(\mathbf{k}_n) \Delta \mathbf{k}_n$ , where  $\Delta \mathbf{k}_n$  is the area of the 'bin' in the wave-vector plane containing the discrete mode  $\mathbf{k}_n$ . For example, in the case of regularly spaced discrete modes separated by  $\Delta k_x$  and  $\Delta k_y$ ,  $\Delta \mathbf{k}_n = \Delta k_x \Delta k_y$ . We define the wave steepness as  $\epsilon = k_p \sqrt{2 \sum_n S_n}$ , where  $k_p$  is the spectral peak wavenumber.

For all the numerical simulations in this paper we have chosen  $S(\mathbf{k})$  as JONSWAP spectra, i.e.

$$S(\mathbf{k}) = \frac{\alpha}{2k^3} \exp \left[ -\frac{5}{4} (k/k_p)^{-2} \right] \gamma^{\exp[-(\sqrt{k/k_p}-1)^2 / (2\sigma_A^2)]} D(\theta), \quad (4.8a)$$

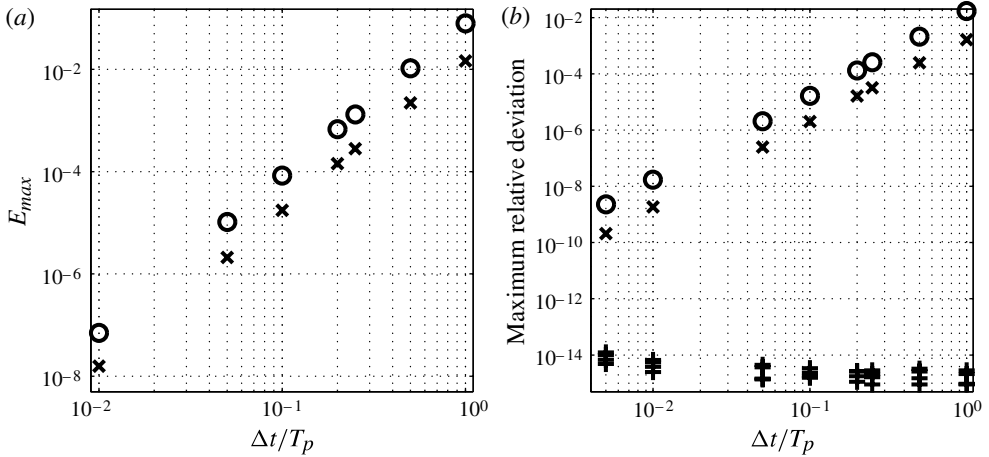


FIGURE 1. (a)  $E_{max}$  as a function of the time step  $\Delta t$  (crosses: one-dimensional (1-D), circles: two-dimensional (2-D)). (b) Maximum relative deviation of invariants: averaged wave action and momentum in 1-D and 2-D (pluses) and averaged Hamiltonian (crosses: 1-D, circles: 2-D).

where  $\mathbf{k} = k(\cos \theta, \sin \theta)$  and where

$$D(\theta) = \frac{1}{k\sqrt{\pi}} \frac{\Gamma(N/2 + 1)}{\Gamma(N/2 + 1/2)} \cos^N \theta \quad (4.8b)$$

in two horizontal dimensions and  $D(\theta) = 1$  in one horizontal dimension. Here,  $\Gamma$  is the Gamma function. The parameter  $\sigma_A$  has the standard values 0.07 for  $k \leq k_p$  and 0.09 for  $k > k_p$ . The parameters  $\alpha$ ,  $k_p$ ,  $\gamma$  and  $N$  are chosen in each case in order to get a desired spectral shape. Note that although the PAE in principle is valid also for finite water depth  $h$ , all the numerical results presented in this paper are obtained for infinite depth  $h \rightarrow \infty$ .

## 5. Numerical validation

In the following we present some testing of the numerical method with respect to the choice of discretization and integration time step. For this testing we have used JONSWAP spectra (4.8) with  $\gamma = 3.3$  and  $\alpha = 0.0238$ , corresponding to a wave steepness  $\epsilon = 0.12$ . In the two-dimensional case  $N = 16$  is used. The integration in time is performed up to  $t_{max} = 1000T_p$ , where  $T_p$  is the period corresponding to the peak wavenumber  $k_p$ . First, we consider the effect of the integration time step  $\Delta t$  by running some simulations with different values of  $\Delta t$ . To check the convergence of the numerical method we define a measure for the difference between two solutions  $C_n(t)$  and  $C_n^{(R)}(t)$ :

$$E_{max} = \max_{0 \leq t \leq 1000T_p} \left( \frac{1}{\epsilon^2} \sum_n |C_n(t) - C_n^{(R)}(t)| \right), \quad (5.1)$$

and let  $C_n^{(R)}(t)$  be a solution obtained by using a very small time step (here  $\Delta t = T_p/200$ ). Figure 1(a) shows  $E_{max}$  for different values of  $\Delta t$  for the one-dimensional (crosses) and two-dimensional (circles) simulations. Consistent with the order of the numerical scheme (4.3),  $E_{max}$  decreases proportional to  $\Delta t^3$ . Figure 1(b)

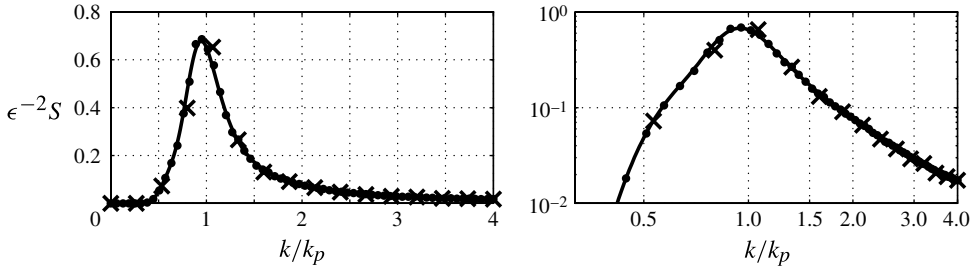


FIGURE 2. One-dimensional spectra in linear and logarithmic scales at  $t = 1000T_p$  for different discretizations:  $n = 16$  (crosses),  $n = 64$  (dots) and  $n = 512$  (solid line).

shows the maximum relative deviation of the invariants (3.1) during the simulations. The averaged wave action and momentum, shown with pluses in the figure, are conserved with very high accuracy independent of the time step. As was brought to our attention by one of the referees, this is because both wave action (for any grid) and momentum (for the regular grid used here) are conserved simply by construction of the algorithm and thus conserved to machine precision independent of time step. For the averaged Hamiltonian (crosses and circles in the figure) accuracy depends on the time step, also here with the expected convergence proportional to  $\Delta t^3$ . All together, the results in figure 1 show that the numerical scheme seems to converge properly and that the global truncation error of  $O(\Delta t^3)$  is verified.

Further we wish to check how the numerical results depend on the discretization of the wavenumber plane. This is performed by running simulations with the same initial condition and time step, but with different resolution of the wavenumber space. Figure 2 shows the final one-dimensional spectrum after  $t = 1000T_p$  obtained by using  $n = 16$ ,  $n = 64$  and  $n = 512$  points to resolve the wavenumber axis on the interval  $[0, 4k_p]$ . It is clear that all three resolutions give similar results, however with some small discrepancies in the  $n = 16$  case. Still the results of figure 2 indicate that the one-dimensional results are quite robust with respect to resolution of the wavenumber axis.

In two dimensions the testing is performed by choosing three different discretizations of the wavenumber plane in the region  $k_x \in [0, 3.5k_p]$ ,  $k_y \in [-1.5k_p, 1.5k_p]$ , where the spectral peak is located at  $(k_x, k_y) = (k_p, 0)$ , namely  $n_x \times n_y = 23 \times 19$  (437 points),  $n_x \times n_y = 30 \times 25$  (750 points) and  $n_x \times n_y = 46 \times 37$  (1702 points). Contour plots of the resulting two-dimensional wave spectra after  $t = 200T_p$  and  $t = 1000T_p$  are shown in figure 3(a,b), while the corresponding directionally integrated spectra at  $t = 1000T_p$  are shown in figure 3(c). We note that the results obtained with the coarsest discretization differ somewhat from the two cases with finer resolution, indicating that a too coarse resolution of the wavenumber plane may produce inaccurate results. Fortunately, the two finest resolutions produce very similar results, suggesting that we have reached ‘stable’ results with respect to the resolution of the wavenumber space. One should note that different from the one-dimensional case, where the spectra remained very smooth throughout the evolution, we here observe some non-smoothness in the spectra after long time evolution. Figure 3 indicates that the amount of noise is somewhat decreased with finer discretization, but this cannot be confirmed without performing simulations with even finer resolution.

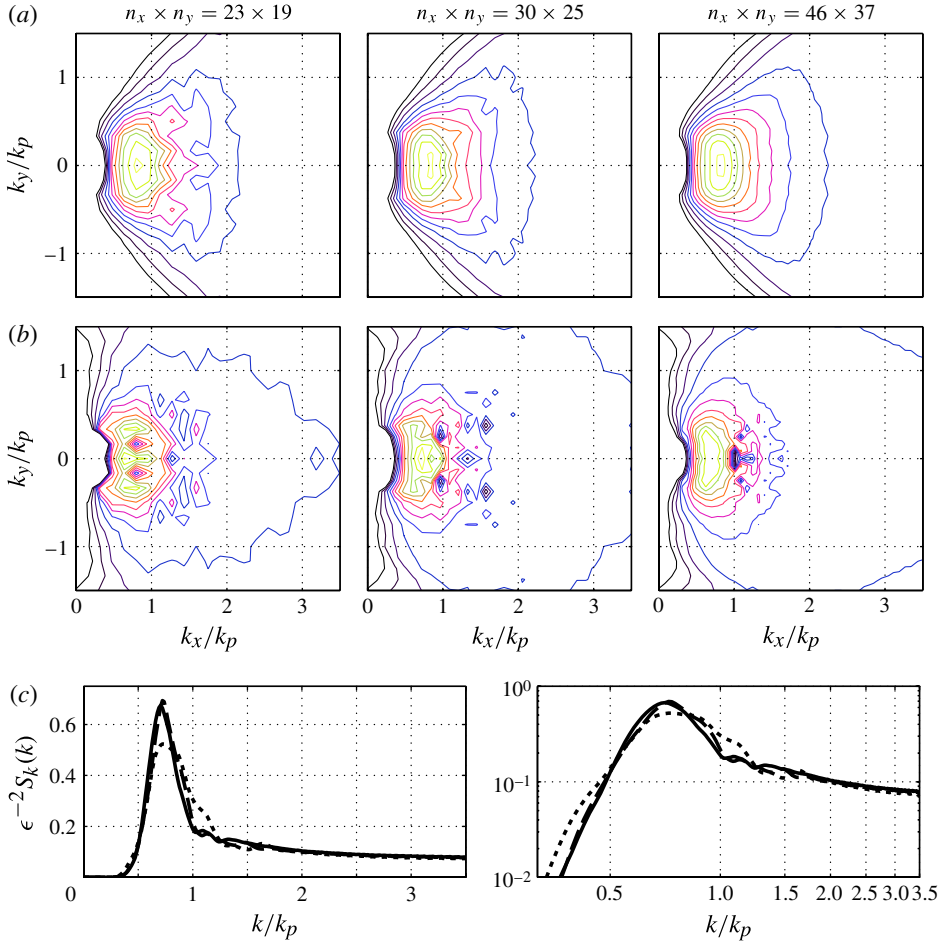


FIGURE 3. (Colour online) Two-dimensional spectra at  $t = 200T_p$  (a) and  $t = 1000T_p$  (b) for the different discretizations. (c) The directionally integrated spectra in linear and logarithmic scales at  $t = 1000T_p$  for  $n_x \times n_y = 23 \times 19$  (dotted line),  $n_x \times n_y = 30 \times 25$  (dashed line) and  $n_x \times n_y = 46 \times 37$  (solid line).

However, due to the large number of interactions in a regular grid we are currently unable to go to finer resolution in the two-dimensional case.

## 6. Evolution of one-dimensional spectra

It is well known that for a one-dimensional spectrum, Hasselmann's kinetic equation predicts no spectral change. This is because exact resonances are absent in one horizontal dimension (Dyachenko & Zakharov 1994). On the other hand, it is also well known that a sufficiently narrow and energetic spectrum will change on a faster time scale not captured by the standard kinetic equation. This is for example verified by numerical (Monte-Carlo) simulations using deterministic equations (see e.g. Dysthe *et al.* 2003; Janssen 2003). It is therefore of interest to see whether the PAE is able to capture this fast spectral evolution. For this purpose we have solved the PAE for three different types of unidirectional JONSWAP spectra with different spectral widths,

Case	$\alpha$	$\gamma$	$\epsilon$
A	0.0364	1.0	0.12
B	0.0238	3.3	0.12
C	0.0083	20.0	0.12

TABLE 1. Parameters of the JONSWAP spectra used in § 6.

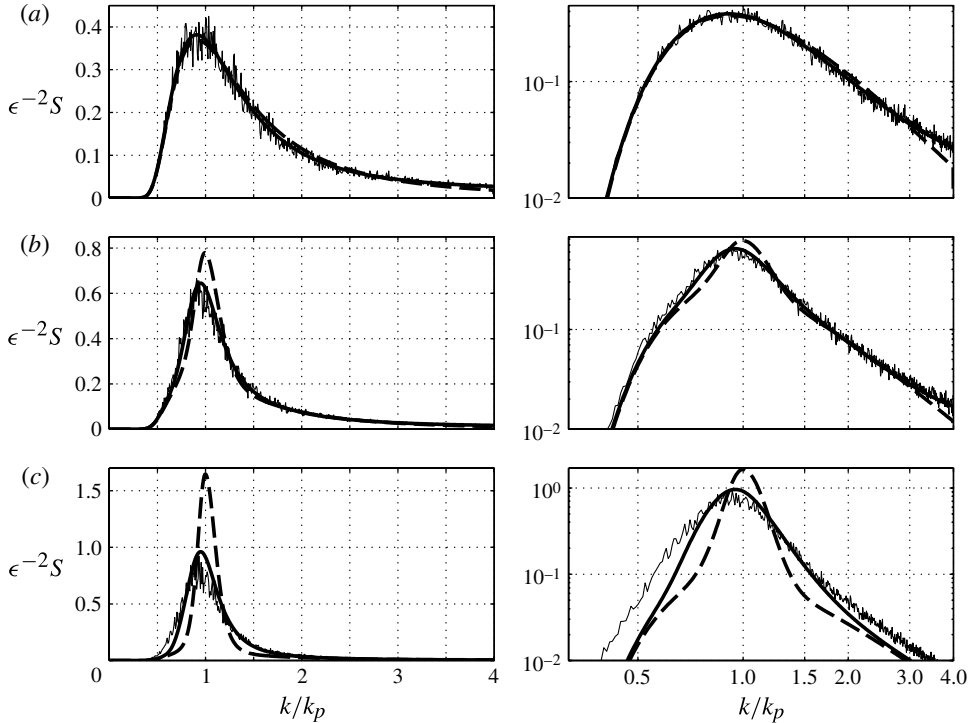


FIGURE 4. Initial spectrum (dashed line) and spectrum after  $1000T_p$  from simulations with the PAE (thick solid line) and Mont-Carlo simulations with the Zakharov equation (thin solid line), in linear and logarithmic scales. (a) Case A ( $\gamma = 1$ ), (b) case B ( $\gamma = 3.3$ ) and (c) case C ( $\gamma = 20.0$ ).

but with the same total energy. The three cases are summarized in table 1. In these simulations, a uniform grid with  $n = 512$  points is used to represent the  $k$ -axis on the interval  $k \in [0, 4k_p]$ . The integration in time is performed up to  $t_{max} = 1000T_p$  with time step  $\Delta t = T_p/2$ .

In figure 4 the spectra obtained from the numerical simulations of the PAE are compared with the corresponding spectra obtained using the Zakharov equation in Monte-Carlo simulations with 100 runs where initial random phases were assigned for each run. The figure shows the spectra after  $t = 1000T_p$ . It is clear that both the PAE and the Zakharov equation predict a broadening of the spectra in the narrower cases ( $\gamma = 3.3$  and  $\gamma = 20$ ). In the broader case ( $\gamma = 1$ ), the spectrum only weakly changes. In all cases there is quite good agreement between the PAE and the Zakharov

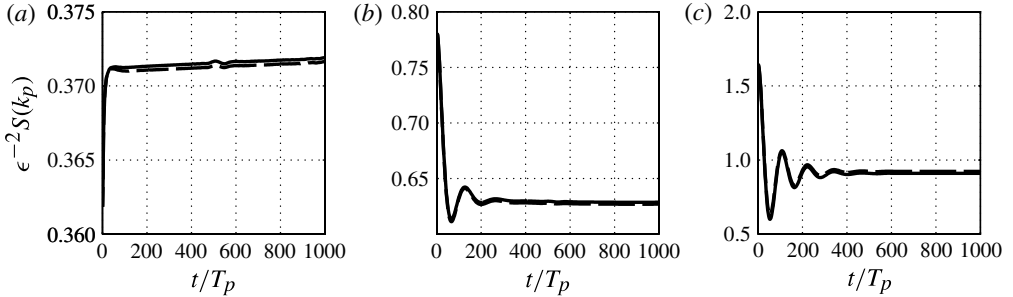


FIGURE 5. Time evolution of the modes corresponding to the spectral peaks obtained from numerical simulations with the PAE, with (broken line) and without (solid line) the contribution from  $\beta_{npqr}$ : (a) case A ( $\gamma = 1$ ); (b) case B ( $\gamma = 3.3$ ); (c) case C ( $\gamma = 20$ ).

equation. Recall that the PAE gives the spectrum directly, while the spectra obtained from the Zakharov equation are results of Monte-Carlo simulations assigning initial random phases in 100 random runs.

The broadening of the spectra takes place during the first 300–400 periods before reaching a practically stable state with no further change. This is illustrated in figure 5 which shows the evolution of the peak modes,  $S(k_p)$ , as a function of time. The existence of a ‘stationary’ state is to a certain extent consistent with the standard kinetic equation, which for a one-dimensional spectrum predicts no spectral change a sufficiently long time after the phases were assumed uncorrelated. For a two-dimensional spectrum one may not expect the existence of such a stationary state, but rather a transition to a slower evolution on the  $O(\epsilon^{-4})$  time scale, as predicted by the kinetic equation for the long time evolution.

In order to check the effect of  $\beta_{npqr}$  in the PAE, we have run the above described simulations both with and without including the contribution from  $\beta_{npqr}$ . The results indicate that the effect of  $\beta_{npqr}$  is relatively minor. This is shown in figure 5, where one sees that the results with and without  $\beta_{npqr}$  are almost identical. We recall from the derivation in § 2 that  $\beta_{npqr}$  arose as an effect of the nonlinear Stokes correction of the frequencies, and is a higher-order effect than other terms in the equation.

## 7. Evolution of two-dimensional spectra

We now turn to the more realistic situation of the evolution of two-dimensional, directional, wave spectra. In principle, numerical simulations of two-dimensional spectra do not introduce additional difficulties compared to the one-dimensional case. However, limitations in computer memory and speed restrict the possible resolution in the spectral space, since the total number of modes now must be distributed over the two-dimensional wave-vector plane. In the following two-dimensional simulations we have used a regular grid with  $n_x \times n_y = 46 \times 37$  points to describe the part of the wave-vector plane  $k_x \in [0, 3.5k_p]$ ,  $k_y \in [-1.5k_p, 1.5k_p]$ , where the spectral peak is located at  $(k_x, k_y) = (k_p, 0)$ . The time step used in the numerical integration is  $\Delta t = T_p$ . As initial conditions we have used JONSWAP spectra in the form (4.8) with  $\alpha = 0.0238$ ,  $\gamma = 3.3$  and three different values for the directional spread parameter:  $N = 4$ ,  $N = 16$  and  $N = 90$ .

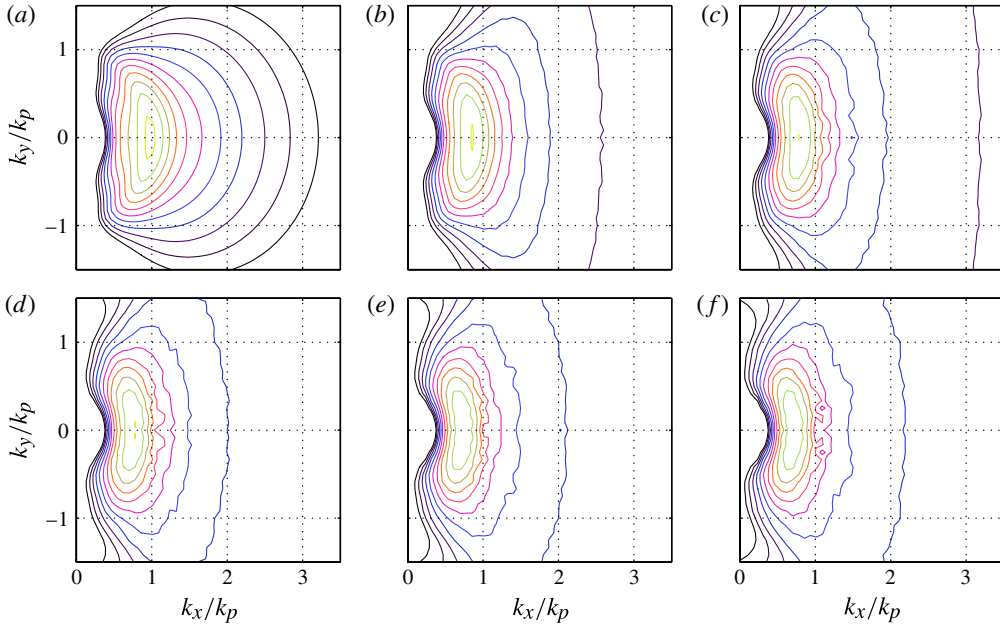


FIGURE 6. (Colour online) Normalized directional spectrum  $\epsilon^{-2}S(\mathbf{k})$  at different times during the evolution for an initial JONSWAP spectrum with  $\alpha = 0.0238$ ,  $\gamma = 3.3$  and  $N = 4$ . The contour levels are chosen as a geometric series with ratio  $10^{0.2}$  between contour levels. The smallest (outermost) contour level has the value  $10^{-2.2}$ . (a)  $t = 0T_p$ ; (b)  $t = 200T_p$ ; (c)  $t = 400T_p$ ; (d)  $t = 600T_p$ ; (e)  $t = 800T_p$ ; (f)  $t = 1000T_p$ .

The directional spectra from the two-dimensional simulations are shown in figures 6–8. Directionally integrated spectra

$$S_k(k) = \int kS(\mathbf{k}) \, d\theta, \quad (7.1)$$

where  $\theta$  is the angle in the  $k_x k_y$  plane, are shown in figure 9.

We observe that during the first part of the evolution, the spectra evolve in a somewhat expected manner, and in qualitative agreement with Monte-Carlo simulations of two-dimensional spectra with random phases assigned initially, using nonlinear Schrödinger-type equations (Dysthe *et al.* 2003). A clear downshift of the spectral peaks is observed in all cases, see e.g. figure 9, a feature which is well established as a main property of the nonlinear evolution of a wave field.

After the relatively strong spectral change during the first 200–400 dominant periods, the spectra seem to only weakly change in the subsequent part of the evolution. This is as expected and similar behaviour is for example reported from Monte-Carlo simulations with the Zakharov equation (Annenkov & Shrira 2006a, 2009). This can also be seen in figure 10, which shows the rate of change of the spectrum defined as

$$\Delta S(t) = \frac{1}{2\epsilon^2} \int |S(\mathbf{k}, t) - S(\mathbf{k}, t + 2T_p)| \, d\mathbf{k}. \quad (7.2)$$

Figure 10 confirms the much stronger spectral change taking place during the first 200–400 dominant periods. It is possible to roughly estimate the time scales of the evolution from figure 10. For very short time, the first few wave periods, the rate of

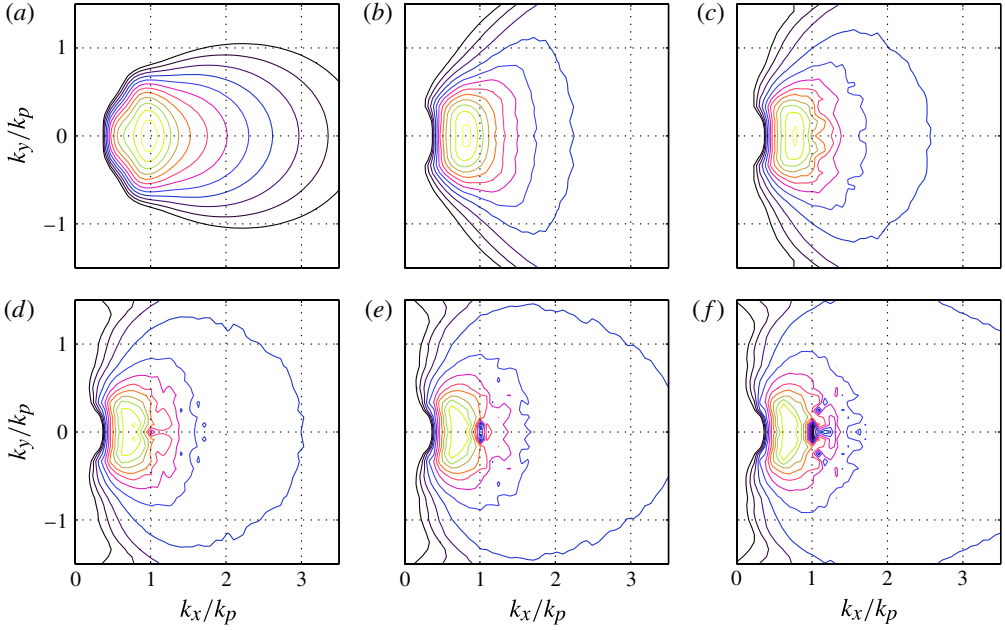


FIGURE 7. (Colour online) Same as figure 6 but for  $N = 16$ .

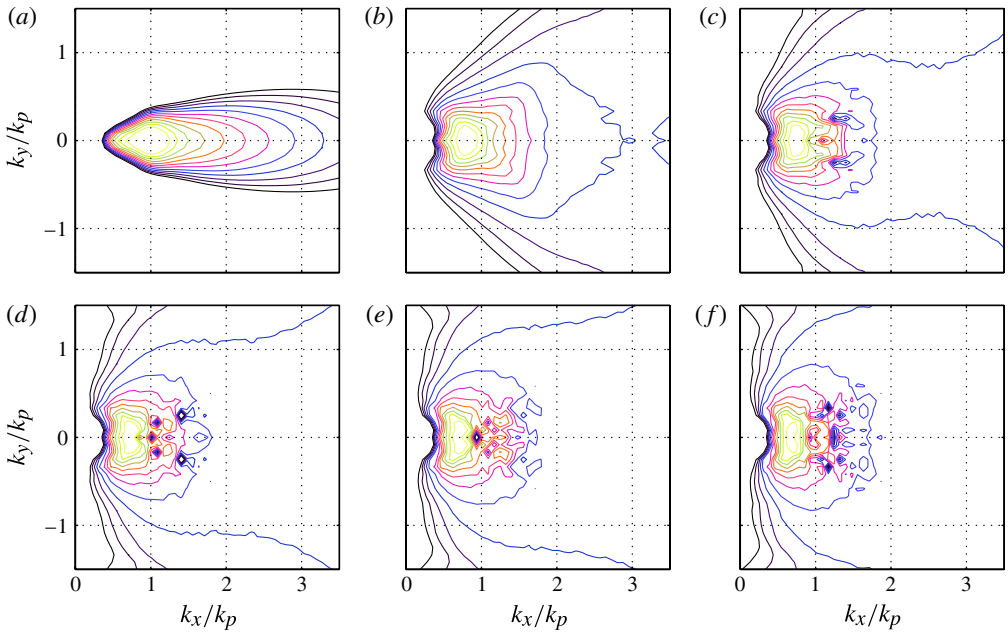


FIGURE 8. (Colour online) Same as figure 6 but for  $N = 90$ .

change is small and in agreement with the  $O(\epsilon^{-4})$  time scale. This is consistent with the short-time asymptotic behaviour of the PAE (Annenkov & Shrira 2006b). After

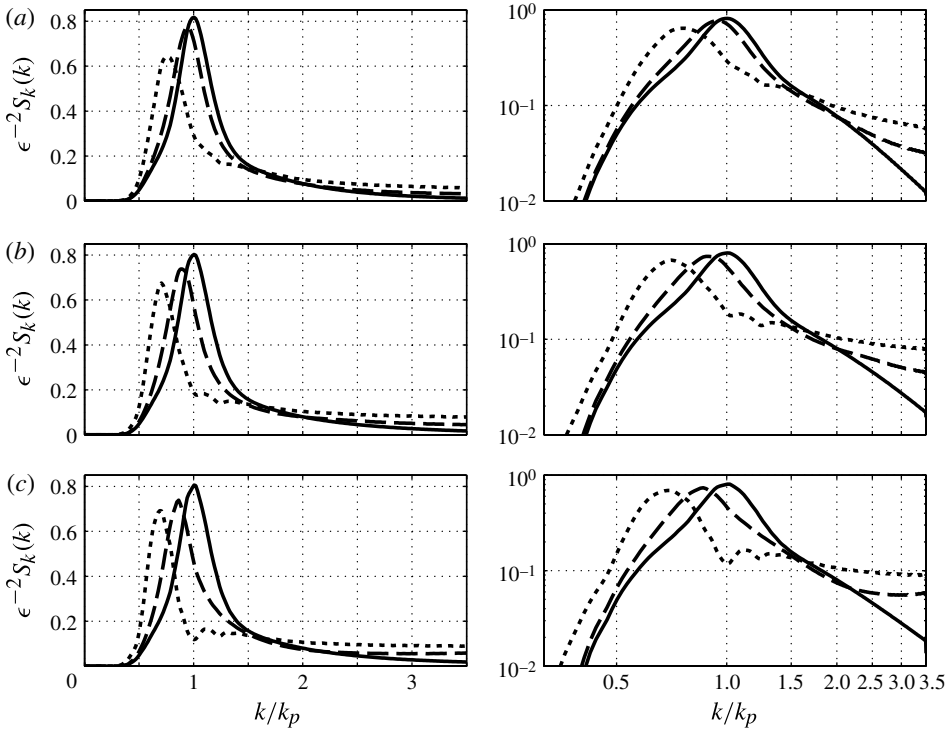


FIGURE 9. Directionally integrated spectra  $\epsilon^{-2}S_k(k)$  in linear and logarithmic scales at  $t = 0$  (solid line),  $t = 100T_p$  (dashed line) and  $t = 1000T_p$  (dotted line). (a)  $N = 4$ , (b)  $N = 16$ , and (c)  $N = 90$ .

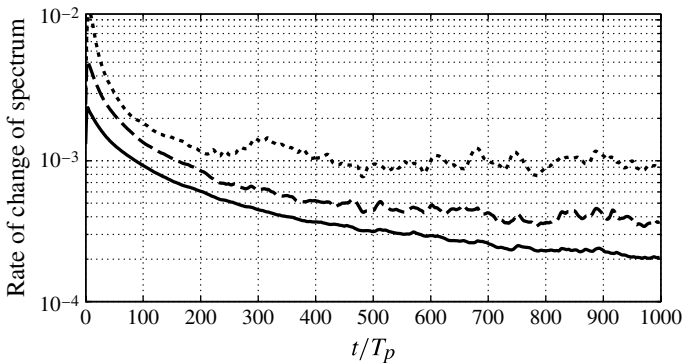


FIGURE 10. Rate of change of spectra,  $N = 4$  (solid line),  $N = 16$  (dashed line) and  $N = 90$  (dotted line).

this very initial stage, there is a period of relatively fast evolution on approximately  $O(\epsilon^{-2})$  time scale. Then again, after a few hundred dominant periods, the rate of change gradually decreases and approaches more or less the  $O(\epsilon^{-4})$  time scale.

For further comparison and validation we have also performed two-dimensional simulations with the Zakharov equation, where 100 simulations with initial random

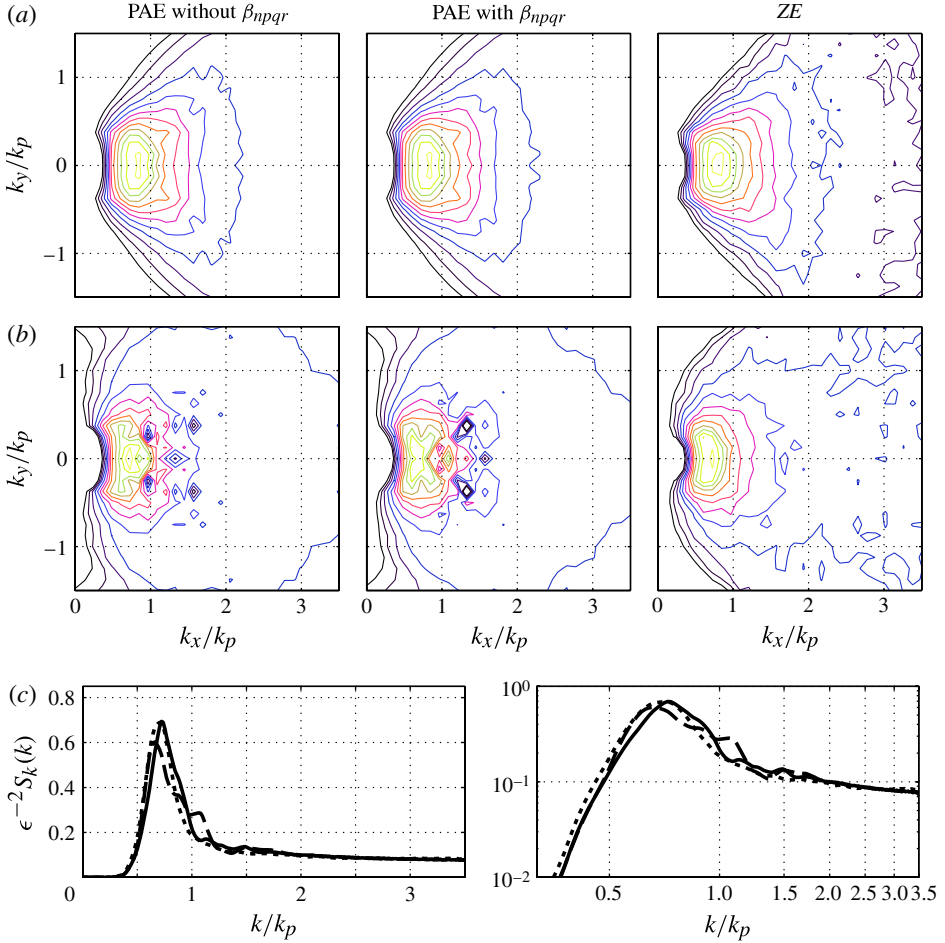


FIGURE 11. (Colour online) Two-dimensional spectra at  $t = 200T_p$  (a) and  $t = 1000T_p$  (b) for PAE without and with the effect of  $\beta_{npqr}$  and for Monte-Carlo simulations with the Zakharov equation. (c) The directionally integrated spectra in linear and logarithmic scales at  $t = 1000T_p$  for PAE without  $\beta_{npqr}$  (solid line), PAE with  $\beta_{npqr}$  (dashed line) and Monte-Carlo simulations with the Zakharov equation (dotted line).

phases were used to calculate the evolution of the wave spectrum. We also compare the results from simulations with the PAE with and without the effect of the Stokes correction term  $\beta_{npqr}$ . For these comparisons we have chosen the initial spectrum with  $N = 16$ . The comparison is shown in figure 11, and shows the spectra at  $t = 200T_p$  and  $t = 1000T_p$  as well as the directionally integrated spectra at  $t = 1000T_p$  for the three cases: PAE without  $\beta_{npqr}$ , PAE with  $\beta_{npqr}$  and Monte-Carlo simulations of the Zakharov equation.

First we note that the effects of the Stokes correction term in the PAE seems to be small, with the qualitative features of the spectra being practically the same both with and without  $\beta_{npqr}$ . There are however some smaller differences in the magnitude and location of the unphysical ‘noise’ that appear in the spectra after long time evolution.

We further note from figure 11 that there is good agreement between the PAE (with or without  $\beta_{npqr}$ ) and simulations directly with the Zakharov equation. Thus, the PAE

seems to capture the spectral evolution in good agreement with deterministic models such as the Zakharov equation. One should note that in both the simulations with the PAE and with the Zakharov equation, see figures 9 and 11, we observe some accumulation of energy at high wavenumbers, resulting in a relatively slow decay of the spectral tails. This can probably be attributed to the absence of dissipation at high wavenumbers, combined with a limited domain in  $k$ -space.

## 8. The effect of phase mixing

In the derivation of the PAE it is assumed that the phases are uncorrelated at  $t = 0$ , i.e. the fourth-order cumulant  $k_{npqr}(t = 0) = 0$ , see (2.17). As seen from the numerical results in §§ 6 and 7, a spectrum with initially uncorrelated phases goes through an evolution on the relatively fast  $O(\epsilon^{-2})$  time scale. Some time after the phases were assumed uncorrelated, this fast evolution of the spectrum ceases, and one observes a further evolution on the much slower  $O(\epsilon^{-4})$  time scale (or no evolution at all in the one-dimensional case).

In the following we want to investigate the effect of ‘re-mixing’ of the phases on the spectral evolution. That is, we imagine the presence of some physical process that uncorrelates the phases at certain times during the evolution. Physically, wave breaking may be an example of such a process (Babanin *et al.* 2007, 2010). It is clear that if phase mixing occurs, this might lead to a quite different field evolution compared to the case where the phases are assumed uncorrelated only in the far past, which is the main assumption in standard kinetic equation.

Within the framework of the PAE, the non-Gaussianity of the wave field is realized through the non-zero value of the fourth-order cumulant  $k_{npqr}$ , see (2.17). Therefore, forcing  $k_{npqr}$  to be zero at some point in the evolution of the PAE is equivalent to resetting the wave field to a Gaussian state, or in other words, mixing/decorrelation of the phases. Hence, what we in the following will refer to as ‘phase mixing’ is accomplished by restarting the PAE, i.e. setting  $t = 0$  and thus setting  $k_{npqr} = 0$ , see (2.17), while keeping the wave action spectrum  $C_n$  unchanged.

In the following numerical simulations where ‘phase mixing’ is applied, we have used the same initial conditions as in §§ 6 and 7. However, at regular time intervals  $T_r$  we now restart the simulations by using the end result  $C_n(t = T_r)$  as the new initial conditions, i.e. we keep the spectrum  $C_n$  but make a new assumption of random phases. Here we have used a regular interval  $T_r = 50T_p$  between each time the phases are mixed. This choice of time interval is quite consistent with findings from numerical simulations of wave breaking by Babanin *et al.* (2007).

In the one-dimensional case the numerical simulations show that, indeed, mixing of the phases leads to quite different long-time spectral evolution compared to the results in § 6, where the phases were assumed uncorrelated only at  $t = 0$ . After each phase mixing, a new period of ‘fast’ evolution takes place, and we therefore do not reach a ‘stationary’ state as seen in § 6. Figure 12 shows the spectra at  $t = 1000T_p$  in the case where the phases have been mixed every  $50T_p$ , compared to the case where phases are not mixed (the results from § 6). It is clear that the phase mixing leads to a stronger change of the spectrum, in particular much stronger downshift of the peaks. Figure 13 shows the evolution of the initial peak mode for the cases with and without phase mixing. We note that although the spectra continue to change as long as the phases are mixed at regular intervals, the rate of change decreases with time, i.e. the rate of change depends also on the spectral shape. In fact, figure 12 may indicate that all spectra converge to some common equilibrium spectrum where there is no further

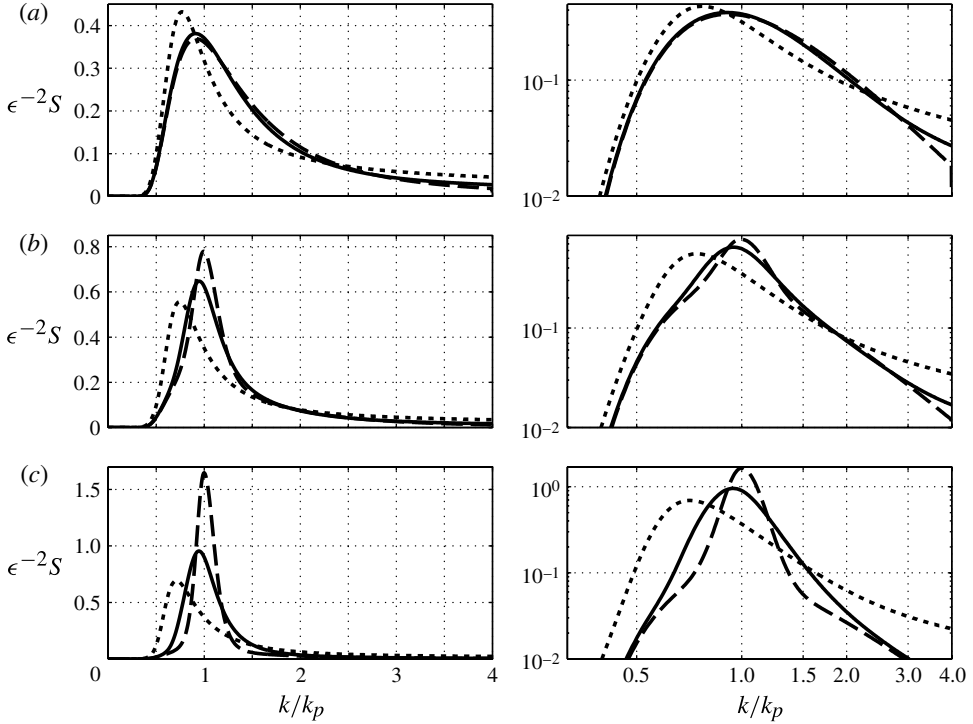


FIGURE 12. Initial spectrum (dashed line) and spectrum after  $1000T_p$  from numerical simulations with (dotted line) and without (solid line) mixing of the phases at regular intervals, in linear and logarithmic scales. (a) Case A ( $\gamma = 1$ ), (b) case B ( $\gamma = 3.3$ ) and (c) case C ( $\gamma = 20.0$ ).

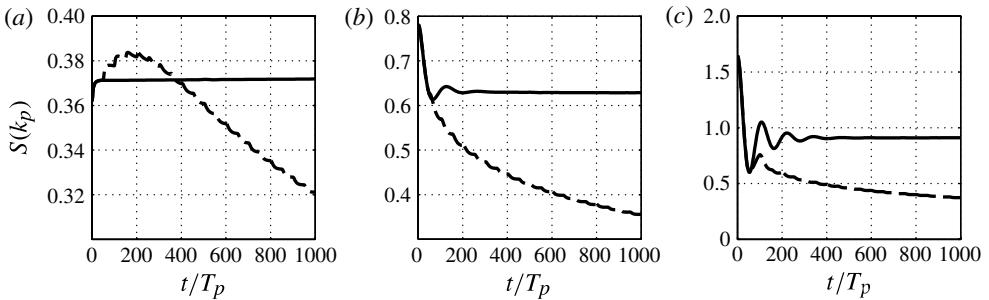


FIGURE 13. Evolution of the modes corresponding to the initial spectral peaks with (dashed line) and without (solid line) phase mixing. (a) Case A ( $\gamma = 1$ ); (b) case B ( $\gamma = 3.3$ ); (c) case C ( $\gamma = 20$ ).

change, even with uncorrelated phases. If such a spectrum does exist it would be a stationary solution to the PAE. Indeed, by looking at the spectra after very long time evolution we see that they are becoming more and more similar, as seen in figure 14, which shows the spectra after  $t = 50\,000T_p$  (with phase mixing every  $50T_p$ ). However the time required to reach a possible common equilibrium state seems to be extremely

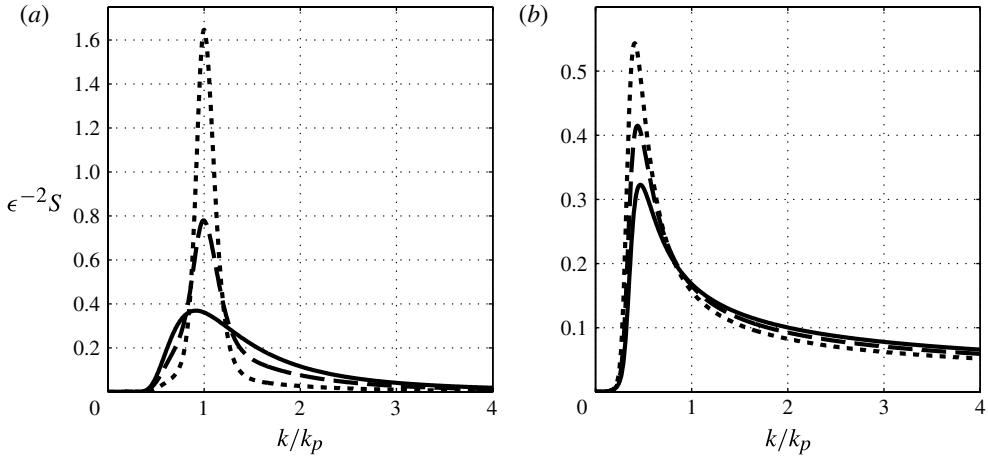


FIGURE 14. Initial spectra (a) and spectra after  $50\,000T_p$  (b) for case A, B and C (solid line, dashed line, dotted line respectively) when phases are mixed every  $50T_p$ .

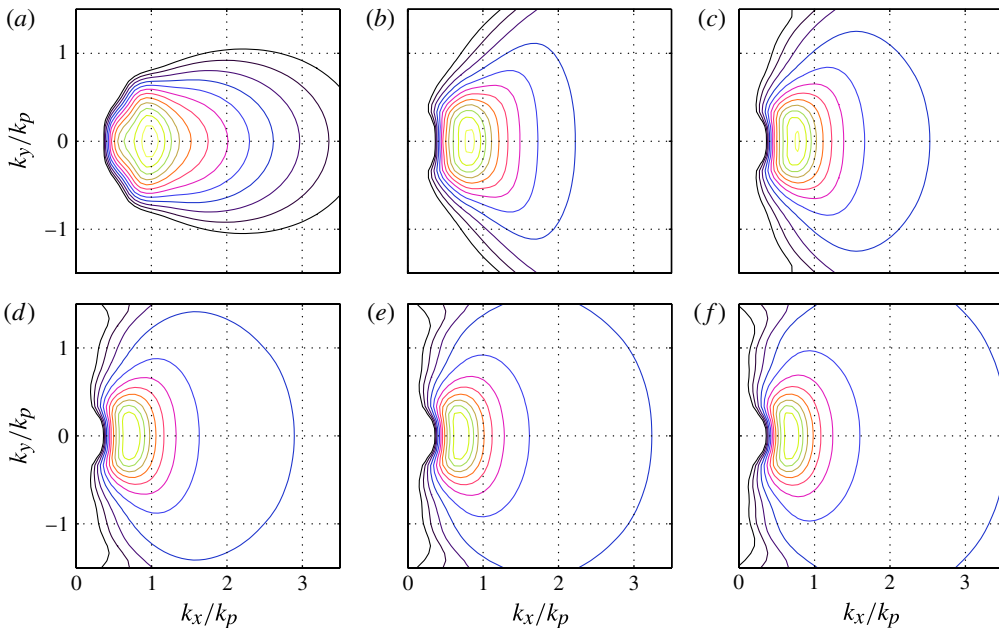


FIGURE 15. (Colour online) Same as figure 6, but for  $N = 16$  and with phase mixing every  $50T_p$ . To be compared with figure 7. (a)  $t = 0T_p$ ; (b)  $t = 200T_p$ ; (c)  $t = 400T_p$ ; (d)  $t = 600T_p$ ; (e)  $t = 800T_p$ ; (f)  $t = 1000T_p$ .

large. Note also that the spectra at  $t = 50\,000T_p$  are rather ‘extreme’, for example with respect to the high-wavenumber part of the spectra, which are proportional to  $k^{-0.6}$  after  $t = 50\,000T_p$  whereas they are proportional to  $k^{-3}$  initially.

We now examine the effects of phase mixing on the two-dimensional results. As an example, the spectral evolution in the  $N = 16$  case is shown in figure 15. We see

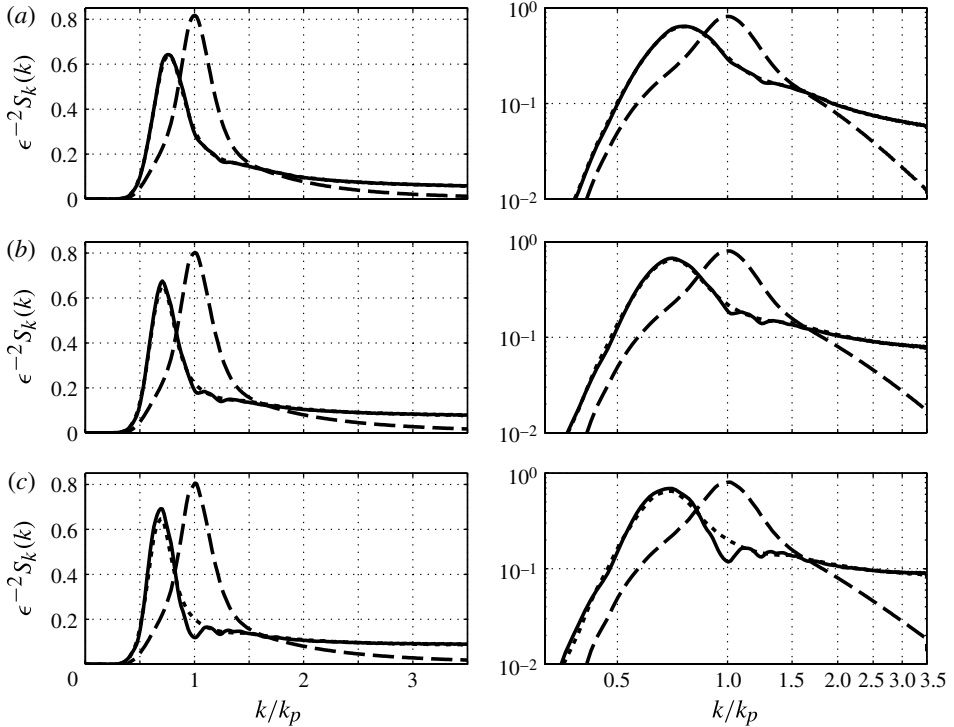


FIGURE 16. Directionally integrated spectra  $\epsilon^{-2}S_k(k)$  in linear and logarithmic scales at  $t = 0$  (dashed line) and at  $t = 1000T_p$  with (dotted line) and without (solid line) phase mixing. (a)  $N = 4$ , (b)  $N = 16$  and (c)  $N = 90$ .

that the spectral evolution is quite similar to the case without phase mixing, except for the minor numerical artifacts seen in the original simulations that we do not have here. The same features are also seen for the other values for  $N$ . Figure 16 shows the directionally integrated spectra at  $t = 1000T_p$  for the results with and without phase mixing. This confirms that the evolutions with and without phase mixing are very similar, different from the one-dimensional case where phase mixing led to a significantly different spectral evolution. Hence, random phases are not sufficient for fast evolution to occur, but that the shape of the spectrum also needs to be sufficiently far from some equilibrium state. Thus, our results indicate that mixing of phases alone is not sufficient to dramatically change the evolution of a two-dimensional spectrum.

## 9. Discussion and conclusions

The main purpose of this work has been to investigate phase-averaged equations that are able to describe evolution on the ‘fast’  $O(\epsilon^{-2})$  time scale. The standard kinetic equation (Hasselmann 1962), which is currently the main model for describing spectral evolution of water waves, is incapable of describing any evolution faster than the slow  $O(\epsilon^{-4})$  time scale. Nevertheless, fast evolution may occur frequently in nature as a result of perturbations that bring a wave field to a state sufficiently far from the near-stationary state predicted by the kinetic equation. Therefore, it is desirable to establish alternatives to the kinetic equation that are able to describe ‘fast’ evolution.

A PAE that is able to capture such fast evolution was proposed by Annenkov & Shrira (2006b). In the present paper we have extended their equation to include some higher-order effects which are related to the nonlinear Stokes corrections of the frequencies. We also present invariants of motion for this PAE. The main part of the paper, however, studies the behaviour of the PAE through numerical simulations, and thereby investigates whether it could have the potential to replace the kinetic equation in situations where fast evolution occurs. Our main findings are summarized and discussed below.

For one-dimensional spectral evolution the PAE is able to predict the evolution in good agreement with Monte-Carlo simulations with the Zakharov equation. The well-known features of spectral broadening and downshift of the spectral peak are reproduced. The results are in contrast to the kinetic equation, which *a priori* predicts no change of a one-dimensional spectrum. However, after the initial stage of the evolution with strong spectral change, the spectra do not change further, consistent with the standard kinetic equation.

Simulations with the PAE in the more realistic case of two-dimensional spectra were also performed with reasonable success. The numerical results agree with known features for two-dimensional spectral evolution and also in two dimensions we find good agreement between the PAE and results from Monte-Carlo simulations with the Zakharov equation. We clearly see the existence and importance of fast  $O(\epsilon^{-2})$  evolution during the initial stages of the evolution.

One should however note that in the two-dimensional simulations we observe some numerical artifacts seen as noise in the spectra, after some time of evolution. These artifacts occur after a few hundred wave periods if the initial spectrum is sufficiently narrow. Although these, relatively minor, artifacts do not seem to dramatically influence the qualitative behaviour of the spectral evolution in the cases we have considered, they may put a limitation on the time range for which we can solve the PAE numerically using the present numerical approach.

We investigated the importance of the new higher-order term in the PAE, which includes effects related to the Stokes nonlinear frequency correction. The numerical results show however that the effect of this term is small both in the one-dimensional and two-dimensional cases that we have examined.

It is also worth noting that the two-dimensional results with narrow directional spreading, e.g.  $N = 90$ , are fundamentally different from the corresponding one-dimensional results. Compare for example the one-dimensional spectra, figure 4, with the directionally integrated two-dimensional spectra in figure 9. Thus, the one-dimensional results are probably not relevant for realistic ocean waves; however, in this paper the one-dimensional simulations have provided convenient numerical test cases.

We further investigated the effects of phase mixing at regular time intervals on the spectral evolution. It is clear that mixing of phases may be one process that may lead to fast spectral evolution. Our findings indicate that for one-dimensional spectra, phase mixing significantly changes the spectral evolution, while for two-dimensional spectra this effect is much weaker, and that phase mixing alone is not sufficient to provoke a dramatically different spectral evolution.

We believe that the present paper clarifies some open questions regarding the description of statistical evolution of water waves. Firstly, we show that the PAE, which was first proposed by Annenkov & Shrira (2006b), can be solved numerically without major difficulties for times up to  $O(10^3)$  wave periods. Previously to the present work no real applications of such modified kinetic equations have been

presented. Secondly, we have established that the PAE indeed has the potential to describe fast spectral evolution of one- and two-dimensional wave fields in qualitative agreement with known features of such evolution. This suggests that the PAE may be a suitable replacement for the kinetic equation in situations where fast evolution may occur, for example in wave forecasting models. Note however that the present work only considers the initial part ( $O(10^3)$  wave periods) of the evolution after a perturbation which leads to fast evolution. However, this is in fact the situation where the standard kinetic equation is not applicable, and where an alternative approach, such as the PAE, is needed.

In the present paper, fast evolution of the spectra occurred as a result of initial spectra that were far from the ‘equilibrium’ predicted by the kinetic equation, in particular due to the assumption of initial random phases. However, it is important to remark that in nature fast evolution may occur for various reasons. In particular it would be desirable to combine the PAE with forcing and dissipation terms and see how, for example, a rapidly varying change of wind forcing affects the spectral evolution on a fast time scale. In general we believe that the PAE has a great potential in future studies and applications.

### Acknowledgements

This work has been supported by the Research Council of Norway through grant 177464/V30 and by the Israel Science Foundation, Grant No. 1194/07. The authors are grateful to Professor V. I. Shrira for his most helpful comments on an early draft of this paper.

### Appendix. Relation to the kinetic equation

In the following we briefly outline how the kinetic equation (Hasselmann 1962) can be derived from the more general PAE. Setting  $\beta_{npqr} = 0$ , the PAE has the form

$$\frac{dC_n}{dt} = 4\text{Re} \sum_{p,q,r} T_{npqr}^2 \delta_{np}^{qr} \exp[i\Delta_{np}^{qr} t] \int_0^t f_{npqr}(\tau) \exp[-i\Delta_{np}^{qr} \tau] d\tau. \quad (\text{A } 1)$$

Now, assuming that  $f_{npqr}$  depends on a slow time scale compared to  $\Delta_{np}^{qr} t$ ,  $f_{npqr}(\tau)$  can be taken outside the integral in (A 1), i.e.

$$\frac{dC_n}{dt} = 4\text{Re} \sum_{p,q,r} T_{npqr}^2 f_{npqr} \delta_{np}^{qr} \int_0^t \exp[i\Delta_{np}^{qr}(t - \tau)] d\tau. \quad (\text{A } 2)$$

In the limit that the fast time  $t \rightarrow \infty$  (in practice this restricts the evolution of  $C_n$  to be on the slow  $O(\epsilon^{-4})$  time scale) the integral yields a delta function of  $\Delta_{np}^{qr}$ , i.e.

$$\frac{dC_n}{dt} = 4\pi \sum_{p,q,r} T_{npqr}^2 f_{npqr} \delta_{np}^{qr} \delta(\Delta_{np}^{qr}), \quad (\text{A } 3)$$

which is the kinetic equation first derived by Hasselmann (1962). For a more detailed derivation of the kinetic equation that follows a similar approach to that indicated above, see e.g. Janssen (2004).

## REFERENCES

- ANNENKOV, S. Y. & SHRIRA, V. I. 2006a Direct numerical simulation of downshift and inverse cascade for water wave turbulence. *Phys. Rev. Lett.* **96** (20), 204501.
- ANNENKOV, S. Y. & SHRIRA, V. I. 2006b Role of non-resonant interactions in the evolution of nonlinear random water wave fields. *J. Fluid Mech.* **561**, 181–207.
- ANNENKOV, S. Y. & SHRIRA, V. I. 2009 Fast nonlinear evolution in wave turbulence. *Phys. Rev. Lett.* **102** (2), 024502.
- BABANIN, A. V., CHALIKOV, D., YOUNG, I. R. & SAVELYEV, I. 2007 Predicting the breaking onset of surface water waves. *Geophys. Res. Lett.* **34** (7)L07605.
- BABANIN, A. V., CHALIKOV, D., YOUNG, I. R. & SAVELYEV, I. 2010 Numerical and laboratory investigation of breaking of steep two-dimensional waves in deep water. *J. Fluid Mech.* **644**, 433–463.
- COOKER, M. J., PEREGRINE, D. H., VIDAL, C. & DOLD, J. W. 1990 The interaction between a solitary wave and a submerged semicircular cylinder. *J. Fluid Mech.* **215**, 1–22.
- DOLD, J. W. & PEREGRINE, D. H. 1986 An efficient boundary integral method for steep unsteady water waves. In *Numerical Methods for Fluid Dynamics II* (ed. K. W. Morton & M. J. Baines). pp. 671–679. Oxford University Press.
- DYACHENKO, A. I. & ZAKHAROV, V. E. 1994 Is free-surface hydrodynamics an integrable system? *Phys. Lett. A* **190** (2), 144–148.
- DYSTHE, K. B., TRULSEN, K., KROGSTAD, H. E. & SOCQUET-JUGLARD, H. 2003 Evolution of a narrow-band spectrum of random surface gravity waves. *J. Fluid Mech.* **478**, 1–10.
- GRAMSTAD, O., AGNON, Y. & STIASSNIE, M. 2011 The localized Zakharov equation: derivation and validation. *Eur. J. Mech. B* **30** (2), 137–146.
- HASSELMANN, K. 1962 On the nonlinear energy transfer in a gravity-wave spectrum. Part 1. General theory. *J. Fluid Mech.* **12**, 481–500.
- JANSSEN, P. A. E. M. 2003 Nonlinear four-wave interactions and freak waves. *J. Phys. Oceanogr.* **33** (4), 863–884.
- JANSSEN, P. A. E. M. 2004 *The Interaction of Ocean Waves and Wind*. Cambridge University Press.
- KRASITSKIL, V. P. 1994 On reduced equations in the Hamiltonian theory of weakly nonlinear surface-waves. *J. Fluid Mech.* **272**, 1–20.
- LVOV, Y. V., BINDER, R. & NEWELL, A. C. 1998 Quantum weak turbulence with applications to semiconductor lasers. *Phys. Nonlinear Phenom.* **121** (3–4), 317–343.
- MEI, C. C., STIASSNIE, M. & YUE, D. K. P. 2005 *Theory and Applications of Ocean Surface Waves, Part 2: Nonlinear Aspects. Advanced Series on Ocean Engineering*, vol. 23. World Scientific.
- PHILLIPS, O. M. 1960 On the dynamics of unsteady gravity waves of finite amplitude. 1. The elementary interactions. *J. Fluid Mech.* **9**, 193–217.
- STIASSNIE, M. & SHEMER, L. 1984 On modifications of the Zakharov equation for surface gravity-waves. *J. Fluid Mech.* **143**, 47–67.
- STIASSNIE, M. & SHEMER, L. 2005 On the interaction of four water-waves. *Wave Motion* **41** (4), 307–328.
- VAN VLEDDER, G. P. & HOLTHUIJSEN, L. H. 1993 The directional response of ocean waves to turning winds. *J. Phys. Oceanogr.* **23** (2), 177–192.
- WASEDA, T., TOBA, Y. & TULIN, M. P. 2001 Adjustment of wind waves to sudden changes of wind speed. *J. Oceanogr.* **57** (5), 519–533.
- ZAKHAROV, V. E. 1968 Stability of periodic waves of finite amplitude on the surface of a deep fluid. *J. Appl. Mech. Tech. Phys.* **9**, 190–194.
- ZAKHAROV, V. E., L'VOV, V. S. & FALKOVICH, G. 1992 *Kolmogorov Spectra of Turbulence*. Springer.